Influence of X and R on the Emission of [Ru(X)(R)(CO)₂(α-diimine)] (X = Halide, Mn(CO)₅; R = Alkyl): Change of Character of the Lowest Excited State from MLCT (X = Cl) to XLCT (X = I) and $\sigma_b\pi^*$ (X = Mn(CO)₅)

Heleen A. Nieuwenhuis,[†] Derk J. Stufkens,[*,†] and Antonín Vlček, Jr.[*,‡]

Anorganisch Chemisch Laboratorium, Universiteit van Amsterdam, Nieuwe Achtergracht 166, 1018 WV Amsterdam, The Netherlands, and J. Heyrovský Institute of Physical Chemistry, Academy of Sciences of the Czech Republic, Dolejškova 3, 182 23 Prague, Czech Republic

Complexes of the type [Ru(X)(R)(CO)₂(α-diimine)], where X = halide or Mn(CO)₅, R = alkyl, and α-diimine = 2,2′-bipyridine (bpy), pyridine-2-carbaldehyde *N*-isopropylimine (iPr-PyCa), and *N,N′*-diisopropyl-1,4-diaza-1,3-butadiene (iPr-DAB), were found to be emissive in 2-MeTHF glass at 77 K. The emission quantum yields are in the 1.3×10^{-2} to 7×10^{-5} range, whereas the lifetimes vary between 15 and 0.3 μs, depending on the ligands. The room temperature emission in fluid solution was investigated for the photostable [Ru(X)(R)(CO)₂-(α-diimine)] complexes (X = halide; R = Me, Et). Emission quantum yields and lifetimes were found to vary in the ranges $1.8 \times 10^{-3} - 10^{-5}$ and 177–40 ns, respectively, according to the nature of X and R. The solution emission of [Ru(I)(Me)(CO)₂(iPr-DAB)] is quenched either by energy transfer (anthracene) or by electron transfer with both electron acceptors (*N,N′*-dimethyl-4,4′-bpy cation or *N*-methyl-4,4′-bpy cation) or donors (amines). Emission properties of this complex are only slightly solvent dependent. In 2-MeTHF solution, both emission quantum yield and lifetime increase with decreasing temperature. Importantly, the nature of the emission (i.e., energy, lifetime, quantum yield, rate constants of both radiative and nonradiative decays) was found to be strongly dependent on the α-diimine ligand used and, especially, on the coligands X and R. However, the nonradiative rate constant does not regularly increase with decreasing emission energy as predicted by the "energy-gap law". Instead, the emission properties were found to reflect the character of the emissive excited state that changes from metal-to-α-diimine charge transfer (MLCT) for X = Cl to halide to α-diimine charge transfer (XLCT) for X = I and σ-bonding to α-diimine ($\sigma_b\pi^*$) for X = Mn(CO)₅.

Introduction

Most investigations of the emission of α-diimine complexes have been concerned with the d⁶ transition metal complexes [Re(L)(CO)₃(bpy)]ⁿ⁺ (n = 0, 1),[1–8] [Ru(bpy)₃]²⁺,[9–16] and their derivatives. These complexes possess rather long-lived metal-to-ligand charge transfer (MLCT) excited states. Much attention has been paid to both inter- and intramolecular energy and electron transfer of these complexes. In particular, the photocatalytic reduction of CO₂, in which [Re(L)(CO)₃(bpy)]ⁿ⁺ is used both as a sensitizer and as a catalyst precursor[17–24] or [Ru(bpy)₃]²⁺ as a photosensitizer,[17,25–30] has been studied in detail.

Photophysical and photochemical properties of such complexes are dependent on the metal, coordinated ligands, temperature, and solvent environment. Therefore, variation of one or more of these factors can be used to tune the excited state properties. In case of the complexes [Re(L)(CO)₃(α-diimine)]ⁿ⁺, the excited state properties are influenced by variation of both L and the α-diimine ligand. For instance, L can act as a bridging ligand to other metal fragments (e.g., CN⁻, 4,4′-bpy)[31–35] or behave as an electron acceptor (e.g., *N*-methyl-4,4′-

† Universiteit van Amsterdam.
‡ Academy of Sciences of the Czech Republic.
⊗ Abstract published in *Advance ACS Abstracts*, July 1, 1995.
(1) Wrighton, M. S.; Morse, D. L. *J. Chem. Soc.* **1974**, *96*, 998.
(2) Stufkens, D. J. *Commun. Inorg. Chem.* **1992**, *13*, 359.
(3) Kalyanasundaram, K. *J. Chem. Soc., Faraday Trans. 2* **1986**, 2401.
(4) Worl, L. A.; Duesing, R.; Chen, P.; Della Ciana, L.; Meyer, T. J. *J. Chem. Soc., Dalton Trans.* **1991**, 849.
(5) Lees, A. J. *Chem. Rev.* **1987**, *87*, 711.
(6) Juris, A.; Campagna, S.; Bidd, I.; Lehn, J.-M.; Ziessel, R. *Inorg. Chem.* **1988**, *27*, 4007.
(7) Sullivan, P. J. *Phys. Chem.* **1989**, *93*, 24.
(8) Van Wallendael, S.; Shaver, R. J.; Rillema, D. P.; Yoblinski, B. J.; Stathis, M.; Guarr, T. F. *Inorg. Chem.* **1990**, *29*, 1761.
(9) Kalyanasundaram, K. *Coord. Chem. Rev.* **1982**, *46*, 159.
(10) Krausz, E.; Ferguson, J. *Prog. Inorg. Chem.* **1989**, *27*, 293.
(11) Ferguson, J.; Herren, F.; Krausz, E. R.; Vrbanich, J. *Coord. Chem. Rev.* **1985**, *64*, 21.
(12) Meyer, T. J. *Acc. Chem. Res.* **1989**, *22*, 163.
(13) Balzani, V.; Barigelletti, F.; De Cola, L. *Top. Curr. Chem.* **1990**, *158*, 31.
(14) Juris, A.; Balzani, V.; Barigeletti, F.; Campagna, S.; Belser, P.; Von Zelewsky, A. *Coord. Chem. Rev.* **1988**, *84*, 85.
(15) Meyer, T. J. *Acc. Chem. Res.* **1989**, *22*, 163.
(16) Meyer, T. J. *Pure Appl. Chem.* **1986**, *58*, 1193.
(17) Hawecker, J.; Lehn, J.-M.; Ziessel, R. *J. Chem. Soc., Chem. Commun.* **1983**, 536.
(18) Kutal, C.; Weber, M. A.; Ferraudi, G.; Geiger, D. *Organometallics* **1985**, *4*, 2161.
(19) Hawecker, J.; Lehn, J.-M.; Ziessel, R. *Helv. Chim. Acta* **1986**, *69*, 1990.
(20) Christensen, P.; Hamnett, A.; Muir, A. V. G.; Timney, J. A. *J. Chem. Soc., Dalton Trans.* **1992**, 1455.
(21) Kutal, C.; Corbin, A. J.; Ferraudi, G. *Organometallics* **1987**, *6*, 553.
(22) Ishida, H.; Terada, T.; Tanaka, K.; Tanaka, T. *Inorg. Chem.* **1990**, *29*, 905.
(23) Pugh, J. R.; Bruce, M. R. M.; Sullivan, B. P.; Meyer, T. J. *Inorg. Chem.* **1991**, *30*, 86.
(24) Tanaka, H.; Nagao, H.; Peng, S.-M.; Tanaka, K. *Organometallics* **1992**, *11*, 1450.
(25) Balzani, V.; Scandola, F. J. *Supramol. Photochemistry*; Ellis Horwood; Chichester, England, 1991.
(26) Hukkanen, H.; Pakkanen, T. *Inorg. Chim. Acta* **1986**, *114*, L43.
(27) Grant, J. L.; Goswami, K.; Spreer, L. O.; Otvos, J. W.; Calvin, M. *J. Chem. Soc., Dalton Trans.* **1987**, 2105.
(28) Denti, G.; Campagna, S.; Serroni, S.; Ciano, M.; Balzani, V. *J. Am. Chem. Soc.* **1992**, *114*, 2944.
(29) Fujita, E.; Milder, S. J.; Brunschwig, B. S. *Inorg. Chem.* **1992**, *31*, 2079.
(30) Belser, P.; Von Zelewsky, A.; Frank, M.; Seel, C.; Vögtle, F.; De Cola, L.; Barigeletti, F.; Balzani, V. *J. Am. Chem. Soc.* **1993**, *115*, 4076.
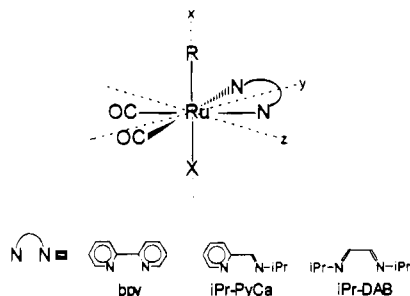
Figure 1. Structure of [Ru(X)(R)(CO)₂(α-diimine)] and the α-diimine ligands used.

bipyridinium)[36] or donor (e.g., 4-(dimethylamino)benzonitrile)[37] in chromophore—quencher (C—Q) complexes. In the latter species, MLCT excitation is followed by an internal electron transfer from the donor to the oxidized metal, resulting in a $[Re^I(L^+)(CO)_3(bpy^-)]^+$ lowest excited state. On the other hand, subtle variations of either α-diimine or L in $[Re(L)(CO)_3(\alpha\text{-diimine})]^{n+}$ which do not alter the character of the lowest excited state have shown that the rate of nonradiative excited state decay decreases (i.e., lifetime increases) with increasing emission energy according to the energy-gap law.[38-41]

In order to introduce similar versatility in the Ru complexes, we have prepared several compounds of the type [Ru(X)(R)-(CO)₂(α-diimine)] (X = halide, Mn(CO)₅; R = alkyl; α-diimine = 2,2′-bipyridine (bpy), pyridine-2-carbaldehyde *N*-isopropylimine (iPr-PyCa) or *N,N′*-diisopropyl-1,4-diaza-1,3-butadiene (iPr-DAB)). The structures of these complexes and of the α-diimine ligands used are depicted in Figure 1.

In a previous article,[42] we have reported the absorption and resonance Raman spectra of these complexes, which clearly showed that variation of X from Cl to I changes the character of the lowest energy transitions from Ru → α-diimine (MLCT) to X → α-diimine (XLCT). Similarly, this change of transition character will influence the excited state properties of these complexes, and this expectation is confirmed by the observed changes in emission energy, lifetimes, and quantum yields reported in this article. For comparison, we have also studied the emission properties of two metal—metal bonded complexes [(CO)₅Mn—Ru(Me)(CO)₂(α-diimine)]. Although the resonance Raman spectra of the latter complexes showed that the lowest energy transitions have MLCT character,[43] crossing to a reactive $\sigma_b(Ru-Mn) \rightarrow \pi^*(\alpha\text{-diimine})$ state was evident from the observed photochemistry.[43] The influence of this $\sigma_b\pi^*$ state on the emission properties is also reported.

Experimental Section

Materials and Preparations. Tetrahydrofuran (p.a.), 2-methyltetrahydrofuran (p.a.), and toluene (UVASOL) were freshly distilled from sodium wire under N₂; dichloromethane and acetonitrile were distilled from CaCl₂. *N,N*-Dimethylformamide was distilled from CaH₂ and stored on molecular sieves (∅ = 4 Å); ethanol was distilled from MgSO₄ and stored on molecular sieves under a nitrogen atmosphere. The complexes were prepared according to literature procedures.[42,43]

Anthracene was used as received, *N,N*-diphenylamine was recrystallized from ethanol/water, and triethylamine was distilled from KOH and stored under nitrogen. *N,N′*-Dimethyl-4,4′-bipyridinium hexafluorophosphate (MV²⁺) and *N*-methyl-4,4′-bipyridinium hexafluorophosphate (MQ⁺) were prepared according to literature methods and recrystallized from acetonitrile/water and acetone/water, respectively.[44]

Absorption and Emission Spectra. Electronic absorption spectra were recorded on either a Perkin-Elmer Lambda 5 or Varian Cary 4E UV—visible spectrophotometer.

Samples for the emission measurements were prepared as optically dilute solutions (ca. 10^{-4} mol dm⁻³) in freshly distilled solvents, which were freeze—pump—thaw degassed at least four times and then sealed under vacuum. Low-temperature measurements were performed in an Oxford Instruments liquid nitrogen cryostat using a cylindrical, glass inner tube of 1 cm diameter as a cuvette. Excitation spectra were recorded on a Spex Fluorolog II emission spectrometer.

Emission spectra, lifetimes, and quantum yields were obtained using a Nd:YAG laser (Spectra Physics GCR-3, 10 ns pulse width) as the excitation source. Samples were excited either at 532 nm using the second harmonic frequency of the Nd:YAG laser or at 460 nm employing a Quanta-Ray PDL-3 pulsed dye laser (Spectra Physics) with coumarin 460 dye pumped by the 355 nm line of the Nd:YAG laser. The emitted light was focused on an optical fiber positioned perpendicularly to the excitation beam and transferred to a spectrograph (EG&G Model 1234) equipped with a 150 g/mm grating and a 250 μm slit, resulting in a resolution of 6 nm. This spectrograph was coupled to a gated, intensified diode array detector (EG&G Model 1421), which is part of an EG&G OMA III handling system, and a 1304 gate pulse amplifier with variable time windows of 100 ns—10 ms or a 1303 gate pulse amplifier with a 5 ns gate window. The programming of the OMA enables one to measure the time-resolved emission spectra at a given time delay after the excitation pulse.

For lifetime measurements at room temperature, the 1303 gate was used, whereas the 100 ns gate of the 1304 was applied at $T \leq 200$ K. The lifetimes were determined from emission spectra measured at 20 different delay times by fitting the emission signal at ten different wavelengths of the emission band to first-order kinetics.

Emission quantum yields (Φ_{em}) were measured using optically dilute solutions relative to a standard solution of Re(Cl)(CO)₃(bpy) ($\phi_s = 0.31 \times 10^{-2}$ at room temperature, $\phi_s = 0.28 \times 10^{-1}$ at 77 K),[4] using the 10 ms gate. Corrections were made according to eq 1,[12,45] in which Φ is the quantum yield of the unknown (u) and standard (s) emitting species, respectively, *I* is the integrated emission intensity, and *A* is the ground state absorbance at the wavelength of excitation (the refractive index $\eta_u = \eta_s = 1$).

$$\Phi_u = \Phi_s \left(\frac{I_u}{I_s}\right)\left(\frac{A_s}{A_u}\right)$$ (1)

The rate constants for radiative (k_r) and nonradiative (k_{nr}) decay are related to Φ_{em} and τ by eqs 2.

$$\Phi_r = \frac{k_r}{k_r + k_{nr}} \qquad \tau = \frac{1}{k_r + k_{nr}}$$ (2)

Results

The emission maxima ($\lambda_{max,em}$), quantum yields (Φ_{em}), and lifetimes (τ) measured for the photostable complexes at room

(31) Schoonover, J. R.; Gordon, K. C.; Argazzi, R.; Woodruff, W. H.; Peterson, K. A.; Bignozzi, C. A.; Dyer, R. B.; Meyer, T. J. *J. Am. Chem. Soc.* **1993**, *115*, 10996.

(32) Tapolsky, G.; Duesing, R.; Meyer, T. J. *J. Phys. Chem.* **1989**, *93*, 3885.

(33) Tapolsky, G.; Duesing, R.; Meyer, T. J. *Inorg. Chem.* **1990**, *29*, 2285.

(34) Kalyanasundaram, K.; Grätzel, M.; Nazeeruddin, Md. K. *Inorg. Chem.* **1992**, *31*, 5243.

(35) Baiano, J. A.; Carlson, D. L.; Wolosh, G. M.; DeJesus, D. E.; Knowles, C. F.; Szabo, E. G.; Murphy, W. R. *Inorg. Chem.* **1990**, *29*, 2327.

(36) Westmoreland, T. D.; Le Bozec, H.; Murray, R. W.; Meyer, T. J. *J. Am. Chem. Soc.* **1983**, *105*, 5952.

(37) Perkins, T. A.; Humer, W.; Netzel, T. L.; Schanze, K. S. *J. Phys. Chem.* **1990**, *94*, 2229.

(38) Caspar, J. V.; Meyer, T. J. *J. Phys. Chem.* **1983**, *87*, 952.

(39) Turro, N. J. *Modern Molecular Photochemistry*; The Benjamin/Cummings Publ. Company, Inc.: Menlo Park, CA, 1978; p 328.

(40) Englman, R.; Jortner, J. *Mol. Phys.* **1970**, *18*, 145.

(41) Kober, E. M.; Caspar, J. V.; Lumpkin, R. S.; Meyer, T. J. *Inorg. Chem.* **1986**, *90*, 3722.

(42) Nieuwenhuis, H. A.; Stufkens, D. J.; Oskam, A. *Inorg. Chem.* **1994**, *33*, 3212.

(43) Nieuwenhuis, H. A.; v. Loon, A.; Moraal, M. A.; Stufkens, D. J.; Oskam, A.; Goubitz, K. *J. Organomet. Chem.* **1995**, *492*, 165.

(44) Luong, J. C.; Nadjo, L.; Wrighton, M. S. *J. Am. Chem. Soc.* **1978**, *100*, 5790.

(45) Parker, C. A.; Rees, W. T. *Analyst (London)* **1960**, *85*, 587.

Table 1. Emission Properties of X/R/α-Diimine in THF at 298 K

| compound	$\lambda_{max,UV-vis}{}^a$	$\lambda_{max,em}{}^a$	τ^b	$10^4\Phi_{em}{}^c$	$10^{-4}k_r{}^d$	$10^{-6}k_{nr}{}^d$	$\Delta E_{(abs-em)}{}^e$
I/Me/iPr-DAB	463, 374	730	177	18	1.0	6	7900
Br/Me/iPr-DAB	449, 334	740	75	3	0.4	13	8758
Cl/Me/iPr-DAB	435	750	63	0.7	0.1	16	9655
I/Et/iPr-DAB	453, 397	747	80	2	0.3	13	8688
Br/Et/iPr-DAB	449, 379	747	40	0.1	0.03	25	8885

^{a} In nm. ^{b} In ns.; estimated error ±5 ns. ^{c} Estimated error 25%. ^{d} In s⁻¹. ^{e} In cm⁻¹.

Table 2. Emission Properties of X/R/α-Diimine in 2-MeTHF at 77 K

compound	$\lambda_{max,UV-vis}{}^a$	$\lambda_{max,em}{}^a$	τ^b	$10^4\Phi_{em}{}^c$	$10^{-2}k_r{}^d$	$10^{-4}k_{nr}{}^d$	$\Delta E_{(abs-em)}{}^e$
I/Me/bpy	390	573	15	130	9	7	8189
I/Me/iPr-PyCa	408, 358	618	10	47	5	10	8329
I/Me/iPr-DAB	410, 350	642	1.8	37	21	55	8814
Br/Me/iPr-DAB	404, 342	648	0.6	6	10	167	9320
Cl/Me/iPr-DAB	387	650	0.3	3	11	384	10455
I/Et/iPr-DAB	405, 355	668	2.2	12	6	45	9721
Br/Et/iPr-DAB	403, 340	672	0.8	2	2	128	9933
Mn(CO)₅/Me/iPr-DAB	529	832	10	0.07	0.007	10	6884
Mn(CO₅)/Me/iPr-PyCa	494	754	11	0.7	0.06	9	6980

^{a} In nm. ^{b} In μs; estimated error ±10%. ^{c} Estimated error 25%. ^{d} In s⁻¹. ^{e} In cm⁻¹.
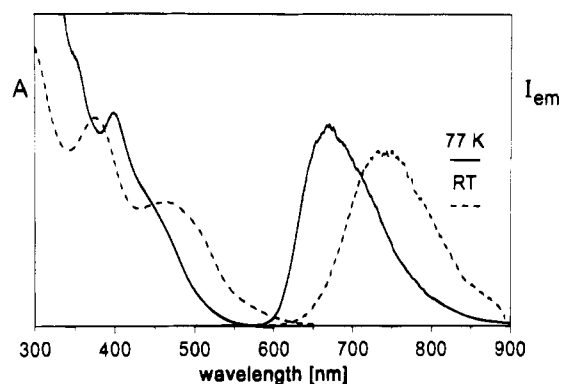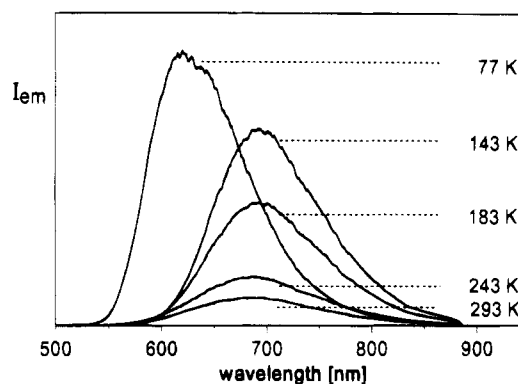

Figure 2. Absorption and emission spectra of I/Me/iPr-DAB in THF at room temperature (dashed line) and in 2-MeTHF at 77 K (solid line).

Figure 3. Temperature-dependent emission spectra of I/Me/iPr-PyCa in 2-MeTHF from 77 to 293 K (1 ms gating time).

temperature and for all complexes under investigation at 77 K are listed in Tables 1 and 2, respectively. Throughout the article, the complexes [Ru(X)(R)(CO)₂(α-diimine)] will be denoted as X/R/α-diimine, e.g., I/Me/iPr-DAB stands for [Ru(I)(Me)(CO)₂-(iPr-DAB)].

The emission bands of all complexes are broad and structureless, even at 77 K in a solid glass, as illustrated in Figure 2. This figure also shows the presence of a large energy difference between the maxima of the emission band and the lowest absorption band, hereafter called apparent Stokes shift, $\Delta E_{(abs-em)}$. Corresponding values are summarized in Tables 1 and 2. Similar large shifts have been observed for analogous Re[I] complexes.[4]

Emission excitation spectra were recorded in the 300−600 nm spectral range for two different complexes in order to establish the origin of the emission. For both I/Me/iPr-DAB and Br/Me/iPr-DAB, the excitation spectra were found to be identical with the absorption spectra, both CT bands being proportionally represented. Also, the emission spectra were independent of the excitation wavelength, which was varied from 355 to 532 nm. These observations show that the emission originates from the lowest excited state, which can be populated either by a direct optical excitation or by an efficient internal conversion from higher CT states.

Temperature Dependence. As shown in Figure 3, the emission of I/Me/iPr-DAB hardly shifts upon lowering the temperature of its solution; it only increases in intensity. Only upon formation of a glass (T < 130 K) does the emission suddenly shift to higher energy due to the increased rigidity of

the medium. At the same time, the emission lifetime increases (Tables 1 and 2). This so-called "rigidochromic" effect, also illustrated in Figure 2, was first observed for some Re[I] complexes[1,5] and later for a series of Ru[II] and Os[II] polypyridyl compounds.[46]

Lumpkin and Meyer have shown that this effect gives rise to a time-dependent shift of the emission maxima in the temperature range of the glass-to-fluid transition, since the lifetime of the excited state is then comparable with the dipole reorientation time.[47,48] Figure 4 shows that the complexes under study behave similarly. At 113 K, at the glass-to-fluid transition region of 2-MeTHF, the emission maximum of I/Me/bpy shifts to lower energy if relatively short gating times are used to monitor the emission.

Emission lifetimes were investigated in fluid solution as a function of the temperature for the complexes I/Me/iPr-DAB and I/Me/iPr-PyCa. Data presented in Table 3 and Figure 5 reveal that the excited state lifetimes decrease with increasing temperature. Experimental data were fitted to the equation $1/\tau = k_o + A\exp(-E_a/RT)$ with correlation coefficients 0.997 (I/Me/iPr-DAB) and 0.980 (I/Me/iPr-PyCa). The following values of the temperature-independent term k_o, preexponential factor A, and activation energy E_a were determined for I/Me/iPr-DAB: $k_o = 1.8 \times 10^6$ s⁻¹, $A = 7.4 \times 10^7$ s⁻¹, and $E_a = 610$

(46) Danielson, E.; Lumpkin, R. S.; Meyer, T. J. *J. Phys. Chem.* **1987**, *91*, 1305.

(47) Lumpkin, R. S.; Meyer, T. J. *J. Phys. Chem.* **1986**, *90*, 5307.

(48) Worl, L. A.; Meyer, T. J. *Chem. Phys. Lett.* **1988**, *143*, 541.
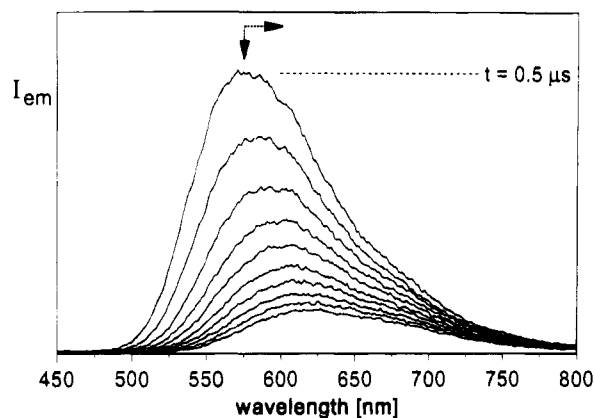
Figure 4. Time-dependent shift of the emission maxima of I/Me/bpy in 2-MeTHF at 113 K with 1 μs delay time between the spectra (100 ns gating time) starting at 0.5 μs after the laser flash.

Table 3. Temperature Dependence of the Lifetimes for I/Me/iPr-DAB and I/Me/iPr-PyCa in 2-MeTHF

T^a	τ (iPr-DAB)^b	τ (iPr-PyCa)^b
143	554	2416
163	454	2038
183	420	1577
203	374	1191
223	320	842
243	275	805
263	226	638
283	199	408
298	180	344

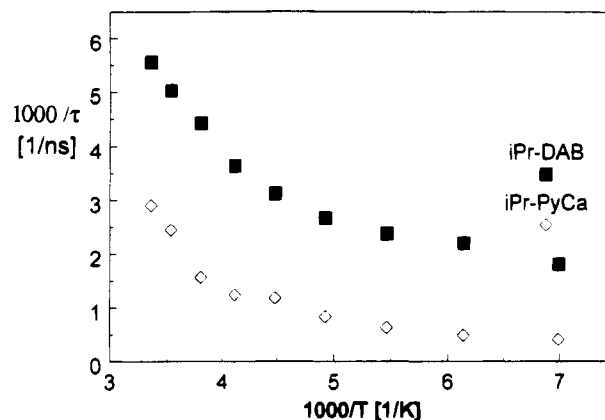^{a} In K. ^{b} In ns; estimated error ± 10 ns.

cm^{-1}. For I/Me/iPr-PyCa: $k_o = 4.8 \times 10^5$ s^{-1}, $A = 2.4 \times 10^8$, and $E_a = 960$ cm^{-1}. The actual dependence appears to involve a temperature-independent term, together with at least two exponentials. The photophysical deactivation pathways were not studied in more detail.

Solvent Dependence. Table 4 shows that, although the positions of the absorption bands are sensitive to the nature of the solvent,[42] the emission maxima and lifetimes of the I/Me/iPr-DAB complex experience only minor solvent influence. Only in acetonitrile are the lifetimes and quantum yields somewhat reduced. This effect appears not to be caused by the polarity of the solvent but by its good coordinating properties, which give rise to a photochemical decomposition of the complexes studied. Similar deviating emission lifetimes and energies in acetonitrile solution have been reported for [Re-(pyr)(CO)₃(substituted-phen)]$^+$ complexes.[8]

Analogous Re(X)(CO)₃(α-diimine) complexes show solvent-independent radiative rate constants. However, their emission lifetimes are shorter in polar solvents, due to the nonradiative rate constants which appear to increase with increasing solvent polarity.[3,50] The absence of any solvent dependence of k_{nr} found for I/Me/iPr-DAB thus indicates that the difference in polarity between ground and excited states is much smaller for the Ru than for the Re complexes, in accordance with the different nature of their excited states.

Quenching Reactions. In order to understand the chemical properties of I/Me/iPr-DAB in its excited state, the emission quenching by anthracene, *trans*-stilbene, *N,N*-dimethyl-4,4'-bpy (MV^{2+}), *N*-methyl-4,4'-bpy (MQ$^+$), triethylamine (NEt₃), and diphenylamine (NHPh₂) was investigated. All these quenchers afford linear Stern—Volmer plots (τ_0/τ_q vs the quencher concentration), indicating thus the bimolecular character of the

(49) Wallace, L.; Rillema, D. P. *Inorg. Chem.* **1993**, *32*, 3836.
(50) Giordano, P. J.; Wrighton, M. S. *J. Chem. Soc.* **1979**, *101*, 2888.

Figure 5. Temperature dependence of emission lifetime and quantum yield for I/Me/iPr-DAB and I/Me/iPr-PyCa in 2-MeTHF.

**Table 4.** Solvent Dependence of the Absorption and Emission Properties of I/Me/iPr-DAB at Room Temperature

solvent	$\lambda_{max, abs}{}^a$	$\lambda_{max, em}{}^a$	τ^b	$10^4 \Phi_{em}{}^c$	$10^{-4}k_r{}^d$	$10^{-6}k_{nr}{}^d$
N,N-dimethyl-formamide	430, 359	712	162	14	0.9	6.2
acetonitrile	436, 360	721	127	10	0.8	7.9
ethanol	440, 365	727	168	16	1.0	5.9
tetrahydrofuran	463, 374	727	177	18	1.0	5.6
dichloromethane	465, 376	729	170	17	1.0	5.9
toluene	485, 386	733	169	21	1.2	5.9

^{a} In nm. ^{b} In ns; estimated error ± 10 ns. ^{c} Estimated error 25%; in s^{-1}.

Table 5. Rate Constants for Quenching of the Emission of I/Me/iPr-DAB by Anthracene, NHPh₂, NEt₃, MQ$^+$, and MV^{2+}

quencher	$10^{-8} \times k_2{}^a$
anthracene ($E_T = 16\,400$ cm^{-1})[39]	1.3
MV^{2+} ($E_{1/2}$(A/A$^-$) = -0.46 V *vs* SCE)[51]	2.8
MQ$^+$ ($E_{1/2}$(A/A$^-$) = -0.96 V *vs* SCE)[52]	1.0
NEt₃ (E_0(D/D$^+$) = 1.02 V *vs* SCE)[54]	0.03
NHPh₂ (E_0(D/D$^+$) = 0.83 V *vs* SCE)[3]	0.07

^{a} M^{-1} s^{-1}.
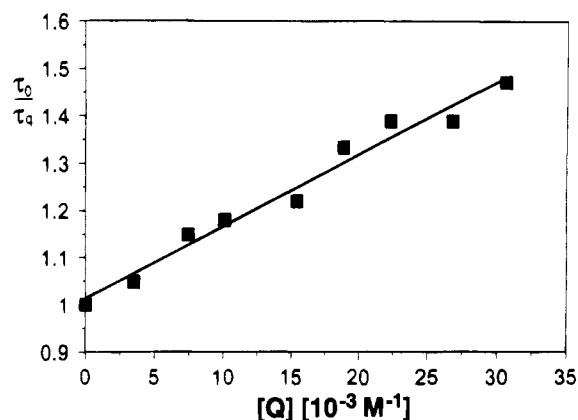
Figure 6. Stern—Volmer plot for the quenching of the emission of I/Me/iPr-DAB by anthracene.

quenching reactions. The bimolecular rate constants k_2 were calculated from the slopes k_q of the Stern—Volmer plots ($k_q = k_2\tau_0$; $\tau_0 = 177$ ns). Their values are summarized in Table 5, together with the quencher redox potentials. For the quenching by anthracene, the Stern—Volmer plot is depicted in Figure 6.

Quenching of the emission of I/Me/iPr-DAB by the typical triplet quencher anthracene ($E_T \cong 16\,400$ cm^{-1})[39] was found to be about 10 times slower than the diffusion. For *trans*-stilbene ($E_T \cong 17\,540$ cm^{-1}), the quenching was unmeasurably

slow. The efficient quenching by anthracene and also by traces of dioxygen points to the spin-triplet character of the emissive excited state of I/Me/iPr-DAB. Comparison between the two quenchers allows us to estimate roughly the zero-point energy of the emissive state as approximately 16 500 cm^{-1}. The excited state energy of I/Me/iPr-DAB thus appears to be smaller than that of [Re(X)(CO)$_3$(bpy)] complexes (X = halide), whose emission was found to be quenched also by *trans*-stilbene although with a smaller rate constant than for the quenching by anthracene.[1] This difference in triplet energy between I/Me/iPr-DAB and Re(X)(CO)$_3$(bpy) is most likely due to the higher energy of the π^*-orbital of bpy as compared to iPr-DAB.

The triplet energies of the other quenchers used are too high (e.g., $E_T \simeq$ 25 000 cm^{-1} for MV^{2+})[51] for an energy transfer from the excited state of I/Me/iPr-DAB. Instead, an oxidative quenching (eq 3) takes place for the electron acceptors (A = MV^{2+}, MQ$^+$):

$$[Ru(I)(Me)(CO)_2(iPr-DAB)]^* + A \rightarrow$$
$$[Ru(I)(Me)(CO)_2(iPr-DAB)]^+ + A^- \quad (3)$$
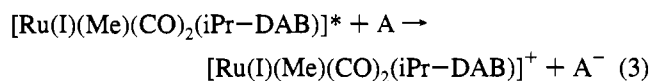
The quenching rate constant for MV^{2+} is somewhat less than diffusion controlled. The quenching rate constant decreased from 2.8 to 1.0 $\times$ 10^8 M^{-1} s^{-1} going from MV^{2+} to MQ$^+$, since MV^{2+} ($E_{1/2}$(A/A$^-$) = -0.46 V vs SCE)[51] is a better oxidative quencher than (MQ$^+$) ($E_{1/2}$(A/A$^-$) = -0.96 V vs SCE).[52] In the ground state, the I/Me/iPr-DAB complex may be electrochemically oxidized. However, this oxidation appears to be coupled with a rapid decomposition of the oxidized product.[53]

During irradiation of the I/Me/iPr-DAB complex in the presence of a higher concentration of either of the electron acceptors, the orange color of the solution irreversibly turned blue. Apparently, the back electron transfer was prohibited by a fast decomposition of the oxidized ruthenium complex. The lability of the oxidized I/Me/iPr-DAB complexes was also established electrochemically.[53]

The reductive quenching by the electron donors (D) NHPh$_2$[3] and NEt$_3$[54] will proceed according to eq 4:

$$[Ru(I)(Me)(CO)_2(iPr-DAB)]^* + D \rightarrow$$
$$[Ru(I)(Me)(CO)_2(iPr-DAB)]^- + D^+ \quad (4)$$
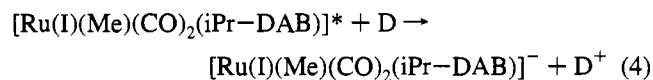
The rate constants of ca. 10^6 M^{-1} s^{-1} are significantly lower than those found for the related Re^I complexes. In comparison, a rate constant of 4 $\times$ 10^8 M^{-1} s^{-1} has been obtained for the quenching reaction of [Re(Cl)(CO)$_3$(bpy)] by NHPh$_2$.[3]

Electrochemical experiments on the ground state of I/Me/iPr-DAB have shown that the reduction product formed upon one-electron reduction (at -1.55 V vs Cp$_2$Fe$^+$/Cp$_2$Fe in THF) undergoes fast chemical reactions.[53]

Influence of Ligands. Tables 1 and 2 show that the emission properties of the complexes strongly depend on the coordinated α-diimine ligand and on X and R.

The emission energy increases when the α-diimine ligand is changed from iPr-DAB to iPr-PyCa and bpy. Similar results have been obtained for related [Re(X)(CO)$_3$(α-diimine)] and [M(CO)$_4$(α-diimine)] (M = Cr, Mo, W) complexes.[4,5,55,56] As

expected, the increase in emission energy is accompanied by a decrease in k_{nr} (i.e., increasing τ). A significant drop in k_{nr} together with a large decrease of the apparent Stokes shift occurs upon going from X/R/iPr-DAB to X/R/iPr-PyCa complexes.

Variation of X (Cl, Br, I) has an unexpected influence on the excited state properties of the X/R/α-diimine complexes, both at room temperature and 77 K. Thus, for the complexes X/Me/iPr-DAB, the emission lifetime at room temperature increases by a factor of 3 upon going from X = Cl to I (Table 1), although the emission maximum does not shift much and the spin$-$orbit coupling increases. The apparent Stokes shift shows a significant decrease in the order Cl > Br > I. An even larger effect on the emission properties is observed when the chloride ion is replaced by the metal fragment Mn(CO)$_5$ (Table 2). Both the absorption and emission maxima then shift strongly to lower energy. The lifetime, however, increases more than 30 times, i.e., opposite to the prediction by the energy-gap law. The apparent Stokes shifts are also significantly smaller for both Mn(CO)$_5$ complexes than for their halide-containing congeners.

Variation of the alkyl group also has a noticeable but irregular influence on the emission properties which cannot easily be ascribed to "energy-gap law" or spin$-$orbit effects. It will be shown hereafter that most of these unexpected changes are due to changes in character of the lowest CT state.

Discussion

Apart from the very unusual influence of the ligand nature, which will be discussed below, the emission of the Ru(X)(R)-(CO)$_2$(α-diimine) complexes exhibits features similar to those characteristic for other organometallic and coordination compounds with emissive M $\rightarrow$ α-diimine CT excited states. The quenching properties and rigidochromic effect are quite typical. The temperature dependence of the emission lifetime measured in fluid solution (Figure 5) indicates the presence of thermally activated excited state deactivation pathways for I/Me/iPr-PyCa and I/Me/iPr-DAB together with a temperature-independent weak coupling to the ground state, characterized by the rate constant, k_0. (The contribution to k_0 from k_r is much smaller and may be neglected; see Tables 1 and 2.) For I/Me/iPr-DAB and I/Me/iPr-PyCa, the thermally activated deactivation pathway was found to be quite significant at 298 K, accounting for 69% and 83%, respectively, of the total rate constant of the nonradiative decay. Previously, the thermally-activated decay of excited states of Re[4] and Os[57] complexes has been ascribed to a thermal population of higher-lying MLCT states (essentially higher members of the emissive MLCT manifold), whereas a reactive dd state is populated in the case of [Ru(bpy)$_3$]$^{2+}$ and its analogues.[58,59] Due to the coordination of strong-field CO and alkyl ligands, the empty d-orbitals of the X/R/α-diimine complexes are expected to lie even higher in energy than for [Ru(bpy)$_3$]$^{2+}$. Hence, the dd states are expected to occur at rather high energy, thermally inaccessible from the lowest CT state. This explains the photostability of these X/R/α-diimine complexes, and the temperature dependence of the excited state lifetime may be best explained by deactivation through a close-lying higher CT state.[4,57] Moreover, the rather large apparent Stokes shift observed for all X/R/α-diimine complexes under study indicates large molecular distortions of the emissive states.

(51) Amouyal, E.; Zidler, B.; Keller, P.; Moradpour, A. *Chem. Phys. Lett.* **1980**, *74*, 314.

(52) Curtis, J. C.; Sullivan, B. P.; Meyer, T. J. *Inorg. Chem.* **1983**, *22*, 224.

(53) Nieuwenhuis, H. A.; Hartl, F.; Stufkens, D. J. to be published.

(54) Dapo, R. F.; Mann, C. K. *Anal. Chem.* **1963**, *35*, 766.

(55) Rawlins, K. A.; Lees, A. J. *Inorg. Chem.* **1989**, *28*, 2154.

(56) Servaas, P. C.; van Dijk, H. K.; Snoeck, T. L.; Stufkens, D. J.; Oskam, A. *Inorg. Chem.* **1985**, *24*, 4494.

(57) Lumpkin, R. S.; Kober, E. M.; Worl, L. A.; Murtaza, Z.; Meyer, T. J. *J. Phys. Chem.* **1990**, *94*, 239.

(58) Durham, B.; Caspar, J. V.; Nagle, J. K.; Meyer, T. J. *J. Am. Chem. Soc.* **1982**, *104*, 4803.

(59) Barigetti, F.; Balzani, V.; Belser, P.; Von Zelewsky, A. *Inorg. Chem.* **1983**, *22*, 3335.

Therefore, it cannot be excluded that a strong coupling between the emissive state and the ground state might also contribute to the observed thermally activated relaxation pathway.[40]

Previous emission studies have shown that the rate of the nonradiative decay of the excited states of most coordination and organometallic compounds follows the energy-gap law,[38,40,41] i.e., that the logarithm of the corresponding rate constant, ln-(k_{nr}), linearly decreases with increasing excited state energy (often approximated by the emission energy) in a homogeneous series of closely related complexes.[60] Such behavior was, e.g., observed for the series of $[Re(L)(CO)_3(bpy)]^{n+}$, $[Rh(NH_3)_5-(L)]^{3+}$, $[Rh_2(CNR)_4(\mu\text{-dppm})_2]^{2+}$, and $[Os(bpy/phen)(L)_4]^{n+}$ complexes[4,5,38,41] when the ligand L or substituent R was varied. These structural variations did, however, change neither the nature of the emissive excited state nor the acceptor vibration-(s).[4,38]

No such general relationship was found for the complexes under study. The only variation that leads to a decrease of k_{nr} with increasing emission energy is the change of the α-diimine ligand. However, replacing iPr-PyCa by iPr-DAB resulted in a much sharper rise of k_{nr} than expected on the basis of the energy-gap law only. Notably, the apparent Stokes shift increases as well. This indicates a larger excited state distortion in case of the iPr-DAB complex, assuming that the triplet—triplet splitting does not change much. This deviation from energy-gap law behavior is not unexpected since the interaction between the metal (d_π) and α-diimine (π^*) orbitals increases on going from the bpy to the iPr-DAB complex, influencing thus the CT character of the emissive excited state.[56,61] As a result, the electron will be transferred to the lowest π^*-ligand-orbital in case of I/Me/bpy, but for I/Me/iPr-DAB, the excited electron will occupy a metal-to-ligand π-antibonding orbital (π^*-d_π). Because of this antibonding character, the lowest excited state of the latter complex is expected to be more distorted, leading to a larger apparent Stokes shift and faster nonradiative deactivation. Accordingly, the temperature-independent excited state deactivation that involves the weak coupling with the ground state, k_o, was found to be 3.65 times faster for I/Me/iPr-DAB than for I/Me/iPr-PyCa. Thus, because of this difference in metal—ligand interaction, the characters of the excited states and the vibronic coupling with the ground state are functions of the nature of the α-diimine ligand. As a result, the energy-gap law cannot be applied anymore to the I/Me/α-diimine complexes.

Contrary to the cases studied previously, e.g., $[Re(L)(CO)_3-(bpy)]^{n+}$, the rate of nonradiative decay of the X/R/α-diimine complexes is either almost independent of the emission energy (X = Cl, Br, I) or depends in a reversed order than predicted by the energy-gap law (R = Me vs Et or X = Mn(CO)_5 vs halide) when either X or R is varied while the α-diimine ligand is kept constant. Thus, variation of X from Cl to I in the complexes X/Me/iPr-DAB causes a strong decrease of k_{nr}, both at room temperature and at 77 K, while the emission energy hardly changes. At the same time, k_r (at 298 K) increases according to expectations, since the spin—orbit coupling increases. A similar behavior is observed for the corresponding X/Et/iPr-DAB complexes. Instead of the emission energy, k_{nr} qualitatively correlates with the apparent Stokes shift. The increase of k_{nr} with increasing apparent Stokes shift appears to be quite general in the complexes investigated. It was found both at 298 and at 77 K within the X/Me/iPr-DAB and X/Et/iPr-DAB.
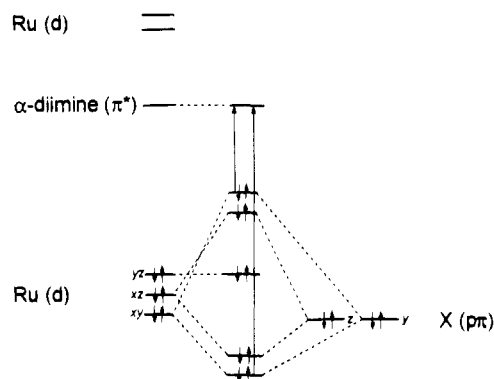

Figure 7. Schematic MO diagram for the complexes X/R/α-diimine.

iPr-DAB series going from I to Br and Cl and when replacing Me by Et in I/R/iPr-DAB and Br/R/iPr-DAB complexes. The $Mn(CO)_5/Me/iPr$-DAB and $Mn(CO)_5/Me/iPr$-PyCa complexes exhibit much lower values of k_{nr} and smaller apparent Stokes shifts than any of their halide analogues.

For the interpretation of these unexpected effects, we have to consider the character of the orbitals involved in the electronic transitions and the nature of the lowest excited states of these complexes. The electronic structure of the complexes may be described by a qualitative MO scheme depicted in Figure 7.[42] The interaction between the halide p_π- and metal d_π- orbitals gives rise to two sets of orbitals having metal—halide bonding and antibonding character, respectively. The emissive lowest-lying excited state originates from electron excitation from the upper ($d_\pi-p_\pi$) antibonding orbital to the π^*-orbital of the α-diimine. As the halide contribution to the ($d_\pi-p_\pi$)-orbital increases when changing X from Cl to Br and I, the nature of the emitting state changes correspondingly from MLCT (X = Cl) to XLCT (X = I).[42] The change of the alkyl ligand from Et to Me has the same effect because of the stabilization of the Ru d_π-orbitals with respect to the X p_π-orbitals. These conclusions are fully supported by the results of our previous study of absorption and resonance Raman spectra.[42] Recently, we have also observed a similar influence of changing X (Cl, Br, I) on the character of the lowest excited state of $[Mn(X)-(CO)_3(bpy)]$ complexes and rationalized this by MO calculations.[62]

The present study shows that, as the emissive excited state becomes increasingly XLCT in character, its nonradiative deactivation becomes slower and the emission exhibits a smaller apparent Stokes shift. The latter observation suggests that the XLCT states are less distorted with respect to the ground states than are the MLCT states, although it can not be excluded that the singlet—triplet splitting is also smaller for the XLCT states. Apparently, the unexpected changes in emission properties upon variation of X and R are directly related to the change of MLCT/XLCT character of the emissive excited state. The vibrational coupling with the ground state is more efficient in highly distorted MLCT states than in XLCT states,[40] providing a more efficient nonradiative relaxation pathway. It is noteworthy that resonance Raman spectra obtained on X/R/α-diimine complexes[42] showed that the Raman band corresponding to the ν_s-(CO) vibration is enhanced in intensity in resonance with the MLCT transition but not with the XLCT transition. Apparently, the MLCT excitation activates the $\nu_s(CO)$ vibration, which acts as an important energy acceptor in the nonradiative deactivation of the MLCT excited states.[4] Such a role of the $\nu_s(CO)$ vibration has previously been established for the deactivation of MLCT-

---

(60) E_{em} need not necessarily follow E_{00} when the Stokes shift is too large. Only for small variations in the studied complexes can E_{em} be applied in the energy-gap law instead of E_{00}.

(61) Stufkens, D. J. *Coord. Chem. Rev.* **1990**, *104*, 39.

(62) Stor, G. J.; Stufkens, D. J.; Vernooijs, P.; Baerends, E. J.; Fraanje, J.; Goubitz, K. *Inorg. Chem.* **1995**, *34*, 1588.

excited [Re(Cl)(CO)₃(bpy)] and related complexes.[4] On the other hand, the lack of enhancement of the ν_s(CO) Raman band in resonance with the XLCT transition suggests that the nonradiative deactivation of the XLCT state does not involve the ν_s(CO) vibration, in accordance with the longer XLCT lifetime, as compared with MLCT. Apparently, the intimate mechanisms of the nonradiative deactivation of XLCT and MLCT excited states are different. Moreover, very large apparent Stokes shifts observed for X/R/α-diimine complexes with lowest excited states of predominantly MLCT character indicate that an additional thermally activated nonradiative relaxation pathway[40] might arise from a strong coupling (i.e., crossing) between potential energy surfaces of the highly distorted MLCT state and the ground state. In accordance with the above explanation, the I/R/iPr-DAB and Br/R/iPr-DAB complexes also exhibit a decrease of k_{nr} with decreasing apparent Stokes shift when changing R from Et to Me, but only in fluid solutions at 298 K. In a low-temperature glass, variation of R in I/R/iPr-DAB influences the k_{nr} much less, although the MLCT character of the excited state increases upon going from R = Me to Et, as manifested by the increase of the apparent Stokes shift (Table 2).

The above-mentioned results show that variation of X and R in [Ru(X)(R)(CO)₂(α-diimine)] has a strong influence on the emission properties of these complexes which can not simply be ascribed to an energy-gap law effect. An even stronger effect is observed when the halide in X/Me/ᶦPr-DAB is replaced by the Mn(CO)₅ group. Because of the electron-donating properties of this group, the first absorption band shifts to lower energy, from 387 to 529 nm at 77 K, when Cl is replaced by Mn(CO)₅ (Table 2). At the same time, the emission shifts from 650 to 830 nm. According to the energy-gap law, such a shift should be accompanied by a decrease of emission lifetime, provided that the character of the lowest excited state does not change. Contrary to this, by replacement of Cl by Mn(CO)₅ in X/Me/ᶦPr-DAB, the emission shifts significantly to lower energy, whereas the lifetime strongly increases! Both k_r and k_{nr} decrease appreciably, indicating that the lowest excited state has changed character in such a way that the probability of the transition to the ground state has become very low.

A comparison of this result with the behavior of related complexes shows that we are dealing here with a more general phenomenon. Thus, replacement of X = Cl by Ph₃Sn in [Re-(X)(CO)₃(phen)] causes the room-temperature emission to shift from 577 to 730 nm, whereas the lifetime increases from 0.3 to 1.8 µs.[1,63] At 77 K, the emission lifetime of Re(X)(CO)₃(phen) even increases from 3.8 to 90 µs when Cl is replaced by Ph₃-Sn, although the emission shifts from 530 to 630 nm.[38]

This difference in character between the lowest excited states of the halide and metal—metal bonded complexes is also reflected in their photochemical behavior. Halide complexes having a lowest nonreactive MLCT (X = Cl) or XLCT (X = I) state are photostable at room temperature, whereas the metal—metal bonded complexes Mn(CO)₅/Me/α-diimine photodecompose into [Mn(CO)₅]• and [Ru(Me)(CO)₂(α-diimine)]• radicals with high quantum yields.[43] Just as for the related complexes [LₙM′—M(CO)₃(α-diimine)] (LₙM′ = (CO)₅Mn, (CO)₅Re, (CO)₄Co, Ph₃Sn; M = Mn, Re), these reactions most probably occur from a $\sigma_b\pi^*$ state, in which an electron has been transferred from the metal—metal bonding orbital (σ_b) to the lowest π^* level of the α-diimine.[61,64,65] On the basis of the analogy between the emission and photochemical behavior of

Mn(CO)₅/Me/α-diimine and of other, previously characterized metal—metal bonded carbonyl α-diimine complexes, we suggest that the emission of Mn(CO)₅/Me/α-diimine originates from the $\sigma_b\pi^*$ state.

Such $\sigma_b \rightarrow \pi^*$ transitions have been observed in the absorption spectra of [Zn(R)₂(α-diimine)] (R = alkyl)[66] and N- or Si-chelate-Irᴵᴵᴵ complexes.[67−69] However, for the Mn(CO)₅/Me/α-diimine complexes under study, as well as for analogous [Re(R)(CO)₃(α-diimine)][70] and [LₙM′—M(CO)₃(α-diimine)][71−73] complexes, the $\sigma_b \rightarrow \pi^*$ transition appears to be at most a minor contributor to the intense absorption band in the visible region. The singlet and triplet $\sigma_b\pi^*$ states can therefore only be populated nonradiatively by a surface crossing with the CT states. The transition probabilities for the deactivation of the $\sigma_b\pi^*$ states to the ground state will also be low. This explains the small values of k_r and k_{nr} found for emission from the ³$\sigma_b\pi^*$ states of the two Mn(CO)₅/Me/α-diimine complexes. Remarkable changes in emission properties on going from Cl/Me/iPr-DAB to Mn(CO)₅/Me/iPr-DAB are therefore explained by different characters of the lowest excited state, ³MLCT (³d$_\pi\pi^*$) and ³$\sigma_b\pi^*$, respectively. This result also implies that the ³$\sigma_b\pi^*$ state of the Mn(CO)₅/Me/iPr-DAB complex is lower in energy than its ³d$_\pi\pi^*$ (MLCT) state. This conclusion is corroborated by the UV-photoelectron spectra of the corresponding complexes [(CO)₅M′-M(CO)₃(iPr-DAB)] (M, M′ = Mn, Re), which showed that the σ_b(M′—M)- orbital has a lower ionization potential than the d$_\pi$(M)-orbitals from which the MLCT transitions originate.[74] This places the ³$\sigma_b\pi^*$ state at lower energy than the lowest ³d$_\pi\pi^*$ (³MLCT) state. The apparent Stokes shifts observed for the Mn(CO)₅/Me/α-diimine complexes are much smaller than those found for the complexes with lowest ³MLCT or ³XLCT states. However, it has a different meaning here. Absorption takes place to a ¹MLCT, since the ¹$\sigma_b\pi^*$ state is not occupied by direct excitation.[43] Emission occurs, however, from the ³$\sigma_b\pi^*$ state. Taking into account that this state is lower in energy than the ³MLCT state, the presence of a small apparent Stokes shift can only imply that the ³$\sigma_b\pi^*$ state is less distorted with respect to the ground state than the ³MLCT state. Also, the distortion of the latter state with respect to the ground state is expected to be smaller for X = Mn(CO)₅ than for X = Cl, as the efficient electron donation from the Mn(CO)₅ group might better compensate the effects caused by the depopulation of the Re d$_\pi$-orbital upon MLCT excitation.

The question remains why the Mn(CO)₅/Me/α-diimine complexes do not decompose from their ³$\sigma_b\pi^*$ state in a glass when this state is so reactive at room temperature.[43] Contrary to the ³$\sigma_b\sigma^*$ state of the metal—metal bonded complexes such as [Mn₂-(CO)₁₀], the ³$\sigma_b\pi^*$ state is not repulsive. Its potential energy curve will have a minimum since one electron still resides in the σ_b(Mn—Ru) orbital while the other occupies a π^*(α-diimine)-orbital not directly influencing the Mn—Ru bond. As a result, there is an activation barrier for the reaction from the

(63) Luong, J. C.; Faltynek, R. A; Wrighton, M. S. *J. Am. Chem. Soc.* **1980**, *102*, 7892.
(64) Meyer, T. J.; Caspar, J. V. *Chem. Rev.* **1985**, *85*, 187.

(65) Stufkens, D. J. *Stereochemistry of Organometallic Compounds;* Bernal, I., Ed.; Elsevier: Amsterdam, 1989.
(66) Kaupp, K.; Stoll, H.; Preuss, H.; Kaim, W.; Stahl, T.; van Koten, G.; Wissing, E.; Smeets, W. J.; Spek, A. L. *J. Am. Chem. Soc.* **1991**, *113*, 5606.
(67) Djurovich, P. I.; Watts, R. J. *Inorg. Chem.* **1993**, *32*, 4681.
(68) Djurovich, P. I.; Watts, R. J. *J. Phys. Chem.* **1994**, *98*, 396.
(69) Djurovich, P. I.; Cook, W.; Joshi, R.; Watts, R. J. *J. Phys. Chem.* **1994**, *98*, 398.
(70) Rossenaar, B. D.; Kleverlaan, C. J.; Stufkens, D. J.; Oskam, A. *J. Chem. Soc., Chem. Commun.* **1994**, 63.
(71) Morse, D. L.; Wrighton, M. S. *J. Am. Chem. Soc.* **1976**, *98*, 3931.
(72) Luong, J. C.; Faltynek, R. A.; Wrighton, M. S. *J. Am. Chem. Soc.* **1979**, *101*, 1597.
(73) Glezen, M. M.; Lees, A. J.; Snoeck, T. L.; Stufkens, D. J. Unpublished results.

$^3\sigma_b\pi^*$ state. This assumption is supported by a recent study of the nanosecond transient absorption spectra of the benzyl complex [Re(benzyl)(CO)$_3$(iPr-DAB)].[70] The results of this study showed that this complex has a rather long lifetime in its $^3\sigma_b\pi^*$ state in apolar solvents (280 ns in toluene) but rapidly decomposes when the weak Re—benzyl bond is affected by an interaction with a solvent molecule. It is also in agreement with our recent observation that the quantum yield for the formation of iPr radicals out of I/iPr/iPr-DAB is strongly dependent on the temperature.[75] This temperature effect is most likely due to a barrier for the homolysis reaction from the σ_b(Ru—iPr)π^* state and not recombination of the radicals, since the quantum yields did not depend on the solvent viscosity.

Conclusion

The [Ru(X)(R)(CO)$_2$(α-diimine)] complexes constitute a new class of emissive organometallic compounds with long-lived excited states of a charge-transfer character. The nature of the emissive excited state and, hence, the emission properties may be finely tuned by the variations in the composition of the coordination sphere, namely by changing the X and R ligands. The character of the emissive state varies from Ru $\rightarrow$ α-diimine ^{3}MLCT (for X = Cl) to X (= I) $\rightarrow$ α-diimine ^{3}XLCT upon variation of X. For X = Mn(CO)$_5$, the emissive excited state was identified as σ(Mn—Ru) $\rightarrow$ π^*(α-diimine), $^3\sigma_b\pi^*$. As a general trend, it appears that both the emission lifetime and

quantum yield decrease in dependence on the emissive state character in the order $\sigma_b\pi^*$ > XLCT > MLCT. This dependence is determined mainly by k_{nr} that increases in the same order, which, however, does not follow the order of decreasing excited state energy. Apparently, the different excited states are coupled to the ground state through different molecular vibrations. The usual dependence of the emission properties on the excited state energy, i.e., the energy-gap law, is thus obscured by the more important dependence on the excited state character.

The quenching experiments performed on [Ru(I)(Me)(CO)$_2$-(iPr-DAB)] complex show that the [Ru(X)(R)(CO)$_2$(α-diimine)] complexes may be considered as energy- or electron-transfer sensitizers. However, their use as excited state oxidants will be limited to stoichiometric processes, due to the inherent instability of their one-electron oxidation products. On the other hand, the [Ru(X)(R)(CO)$_2$(α-diimine)] complexes might find use as sensitizers and/or catalysts in photochemical reductions, especially if the chemistry of their reduction products[53] is further developed toward the activation of reaction substrates.

(74) Andréa, R. R.; Stufkens, D. J.; Oskam, A. *J. Organomet. Chem.* **1985**, *290*, 63.

(75) Nieuwenhuis, H. A.; van de Ven, M. C. E.; Stufkens, D. J.; Oskam, A.; Goubitz, K. *Organometallics.* **1995**, *14*, 780.